RSC Advances

PAPER

View Article Online
View Journal | View Issue

Cite this: *RSC Adv.*, 2024, **14**, 30529

Intricacies of CO_2 removal from mixed gases and biogas using polysulfone/ZIF-8 mixed matrix membranes – part 1: experimental†

Shweta Negi and Akkihebbal K. Suresh *

In this work, we explore the potential of polysulfone/ZIF-8 mixed matrix membranes (MMMs) for the enrichment of biogas to biomethane. To this end, we present data for these MMMs on permeability and selectivity as function of pressure and feed composition, at different loadings of ZIF-8. Specifically, we study dense polysulfone membranes prepared by solvent evaporation, with a ZIF-8 loading in the range 0.5–5 wt% for separation of CO_2 from artificial mixtures of CO_2 and CH_4, and also biogas from an operating plant. The MMMs with 1 wt% filler loading gave the highest enhancement in permeability and selectivity, of 56.8% and 41% respectively, as compared to pure PSF membranes. At higher loadings, a tendency for the ZIF-8 particles to agglomerate was seen, which may compromise the ability of the filler to improve membrane performance. With mixed gases, increases in CO_2 permeability of about 8 to 34% were observed depending on the gas composition, the enhancement being the higher, the lower the CO_2 content. For biogas, permeability and selectivity of the 1% ZIF-8 loaded MMMs were found to be 14.6% and 39.64% lesser respectively than the pure gas values. The study thus throws light on the differences in membrane performance with mixtures as compared to ideal values obtained with pure gases and hence underlines the importance of lab-scale testing of the membranes with actual gas mixtures in the intended applications.

Received 19th June 2024
Accepted 12th September 2024

DOI: 10.1039/d4ra04477k

rsc.li/rsc-advances

1. Introduction

Renewable gases like biogas and landfill gas are being positioned as alternatives to conventional fuels such as natural gas due to their zero carbon footprint and ease of availability.[1,2] While these gases have CH_4 as a major component, the presence of significant amounts of CO_2 lowers their calorific value and hampers their use as an efficient fuel. Various technologies, such as absorption, adsorption, cryogenic separations and membrane separations, are therefore used for separation of CO_2.[3–6] In particular, membrane separation has been successfully employed for CO_2/CH_4 separations in the past few decades. Compared to other techniques, it has a simple configuration, requires low maintenance and has low energy demands;[7,8] it can also be scaled up easily without loss of efficiency.[9] Early research on gas separations was mostly on dense polymeric membranes as they were easy to fabricate and gave a good idea of permeability and selectivity of the polymer used. The ease of membrane formation and its good performance for separation of gases, resulted in vigorous research in this area and an empirical, inverse correlation between permeability and selectivity was shown by Robeson in 1991, based on data available at the time; this came to be regarded as an "upper bound"[10] for membranes. Such data for CO_2/CH_4 separations showed glassy polymeric membranes to possess high permeability and selectivity. Subsequent efforts directed to improve membrane performance resulted in a shift in upper bound in 2008 (ref. 11) for most gas pairs including CO_2/CH_4.

Among materials regarded as the most promising for crossing the Robeson bounds are mixed matrix membranes (MMMs), which have suitable fillers embedded in a pure polymer matrix. MMMs exploit the permeability of both the pure polymer and filler material, resulting in an enhanced permeability. The most important aspect with MMMs is the selection of a suitable filler – it should (a) be compatible with the polymer in order to avoid undesirable features like void formation or rigidification at the polymer–particle interface and (b) assist in the separation, either based on selective affinity or size-exclusion because of pore size. The first report on MMMs dates to 1973 when Paul and Kemp[12] developed membranes using PDMS and 5A zeolites and studied the effect on diffusion time lag. For CO_2/CH_4 separation, the most used fillers are zeolites, metal nanoparticles, silica-based fillers, carbon molecular sieves and metal–organic frameworks (MOFs). These have been discussed in detail in various reviews.[13,14] MOFs consist of inorganic parts connected with organic linkers to form a porous framework with pore size tunability, high

Department of Chemical Engineering, IIT Bombay, Powai, Mumbai 400076, India. E-mail: aksuresh@iitb.ac.in

† Electronic supplementary information (ESI) available. See DOI: https://doi.org/10.1039/d4ra04477k

adsorption capacity and surface area. The organic part present in the MOFs provide for a good interaction between polymer and fillers. The MOFs that are found to show good performance for CO_2/CH_4 separation are ZIFs (Zeolitic Imidazolate Frameworks) that include ZIF-7, ZIF-8, ZIF-11, ZIF-90, ZIF-71, ZIF-108, ZIF-302; UiO (University of Oslo)-66 and MILs (Materials Institute Lavoisier) that include MIL-53(Al), MIL-68(Al), MIL-101(Cr), and MIL-125(Al).[15] Sorribas *et al.* (2014) used silica–ZIF-8 spheres as filler in a polysulfone matrix and found that the CO_2 permeability increased by 300% compared to that of pure membranes.[16] Nuhnen *et al.* 2020 synthesized polyimide membranes with MIL-101(Cr) and MOF-199 as fillers and found that both the selectivity and permeability were higher than the pure membranes.[17] Ahmed *et al.* (2018) used UiO-66 as filler in 6-FDA-DAM polyimide membranes. There has also been interest in amine-functionalised MOFs as fillers in MMMs.[18] Thus, Rodenas *et al.* (2014) used NH_2-MIL-53(Al) and NH_2-MIL-101(Al) for development of MMMs within PSF polymer matrix and found an increase in both the selectivity and CO_2 permeability.[19] Wu *et al.* have used a dual interface engineering approach that led to better compatibilization polymer–particle interface resulting in increased permeability and selectivity for CO_2/CH_4 separations.[20] The high permeability and selectivity in MOF containing MMMs is mainly due to the fact that the adsorption capacity of the MOF for CO_2 is higher than that for CH_4. In some MOFs, size sieving is also responsible for increased selectivity, because the pore size of MOF can be chosen to be between the kinetic diameters of the gases to be separated.

ZIF-8 is a MOF that has good permeability and selectivity for CO_2/CH_4 separations. The high CO_2 permeability in ZIF-8 is due to its higher affinity for CO_2 than CH_4; also, its pore size of 3.4 A is in between the kinetic diameters of CO_2 (3.3 A) and CH_4 (3.8 A). There are several studies in literature on the use of ZIF-8 as a filler in MMMs in both asymmetric and dense membranes. Table 1 summarises the studies on ZIF-8 as a filler in MMMs for CO_2/CH_4 separation. In each case, the table compares the result with the filler with that for the neat polymer. An increase in selectivity for the MMM is reported in all these cases; while in some cases, this increase is at the cost of a decrease in permeability, in others, both permeability and selectivity have been seen to increase.

An analysis done on MMMs shows that the intent of the studies was to establish ZIF-8 nanoparticles as an efficient candidate to enhance the membrane permeability, selectivity or both. The experimentation in these studies has usually been limited to one pressure, and to pure gases.[21–23,25,26] While Ahmad *et al.* (2018) do report studies on equimolar mixture of CO_2 : CH_4, a comparison of performance with pure gases is not available. There is thus a research gap on the performance MMMs with mixed gas feeds. The literature on pure polysulfone membranes suggests that competitive sorption effects could be important in the case of mixed gases with the permeabilities being lower than with the pure components.[26,27] The present study is undertaken to bridge this gap.

The present study is targeted towards determining the gas separation properties of pure PSF and PSF/ZIF-8 MMMs using pure gases as well as gas mixtures, over a range of pressures. Mixtures of CH_4 and CO_2 in different ratios are used as a feed to MMMs and a comparison is made with the pure PSF membranes. Real biogas from an operating biogas plant is also used to establish the efficacy of MMMs in separation of CO_2 from biogas. It is hoped that such a study would enable a rational assessment of the potential of PSF/ZIF-8 MMMs for biogas (or landfill gas) enrichment.

2. Experimental

2.1 Materials used

Polysulfone (P-3500) (Solvay) and polydimethylsiloxane (PDMS) – Sylgard (Sigma-Aldrich), zinc nitrate hexahydrate (Sigma-Aldrich), methyl imidazole (MeIM, Sigma-Aldrich), *N*-methyl pyrrolidone (NMP, Sigma-Aldrich), tetrahydrofuran (Sigma-Aldrich), ethanol (Sigma-Aldrich), chloroform ($CHCl_3$) and water were used in the synthesis of membranes. Polysulfone was dried for 24 hours before use in a hot air oven. All the other chemicals were used as received without further purification.

2.2 ZIF-8 preparation

ZIF-8 was prepared using the method reported in ref. 28. Typically, 1.46 g of $Zn(NO_3)_2 \cdot 6H_2O$ was dissolved in 100 ml of methanol under constant stirring. The resulting solution was added to a solution of 3.24 g of MeIM in 100 ml methanol, and the mixture kept stirred for 1 hour. The resulting milky white solution was centrifuged and washed with methanol 3 times to ensure complete removal of unreacted solute, followed by drying at 70 °C for 12 hours. The resulting particles were ground in a mortar and pestle and stored in a desiccator for further use.

2.3 Membrane preparation

2.3.1 Dope solution preparation. The polymer dope solution was prepared by dissolving PSF (13 wt%) in chloroform (87 wt%) as follows. The required quantity of ZIF-8 (0.5, 0.75, 1, 2 or 5 wt% of the polymer) particles were dispersed in $CHCl_3$ using sonication bath. The dispersion was stirred overnight to ensure uniform dispersion of the nanoparticles. Polysulfone (10% of the required weight) was then added to the dispersion under stirring. After complete dissolution of PSF, the solution was sonicated for 30 min for proper binding between the polymer and particles. This was followed by addition of another 10% polymer to the solution and the process was repeated till all the polymer was dissolved completely. The solution was then stirred overnight to ensure homogeneity of the solution and then degassed for 1 hour in an ultrasonic bath for removal of microbubbles. The degassed solution was kept still for 24 hours for the complete elimination of any trapped bubbles. A similar procedure was followed to prepare the dope solution for nascent membrane without the addition of filler.

2.3.2 Membrane casting. Dense membranes, with different loadings of ZIF-8, were prepared by solvent evaporation technique. The dope solution was spread on a glass plate using a doctors' blade to a thickness of 200 μm. The glass plate was then covered using a glass Petri-dish for uniform and slow

Table 1 Literature showing the work on ZIF-8 MMMs for CO_2/CH_4 separations[a]

Reference	Polymer	ZIF-8 loading (weight%)	CO_2 permeability (barrer)	CO_2/CH_4 selectivity
Bushell *et al.* 2013 (ref. 21)	PIM-1	0	4390	14.2
		28[b]	4270	18.6
Nordin *et al.* 2014 (ref. 22)	Polysulfone	0	25.7[c]	19.43
		5	15.60[c]	28.50
Nordin *et al.* 2015 (ref. 23)	Polysulfone	0	21.2[c]	19.43
		0.5	29.22[c]	23.16
Ahmad *et al.* 2018 (ref. 18)	6FDA-bisP polyimide	0	35.3[d]	25.6
		17	47.7[d]	29.1
Khan *et al.* 2020 (ref. 24)	Polysulfone[e]	0	38.58	20.14
		0.5	47.75	25.70
Sasikumar *et al.* 2021 (ref. 25)	Polysulfone[e]	0	29.64	13.78
		0.5	41.15	22.25

[a] All the data is for flat sheet membranes using pure gases unless indicated otherwise. [b] Volume%. [c] Permeance in GPU. [d] Mixed gas (50 : 50-CO_2 : CH_4). [e] Hollow fiber.

removal of the solvent to ensure homogeneity and left in ambient air. After 24 hours, the membranes were peeled off from the glass plate and dried for 12 h in vacuum oven at 80 °C for complete removal of solvent. In what follows, the membranes with 0.5, 0.75, 1, 2 and 5 wt% loading of ZIF-8 have been designated as DZ0.5, DZ0.75, DZ1, DZ2 and DZ5 respectively.

2.4 Characterization

2.4.1 ZIF-8 and membrane morphology. The purity and the size of the ZIF-8 nanoparticles were determined using XRD analysis carried out on an Empyrean Panalytical Diffractometer. The analysis was done in the 2θ range of 5–50° with radiation of 1.5 Å from a CuKα source. A JEOL-JSM 7600F Field Emission Scanning Electron Microscope (FEGSEM) was used to obtain particle shape and size, for which the particles were carefully spread on a carbon tape placed on an aluminium stub. NETSCHZ STA Luxx analyser was used for determining the

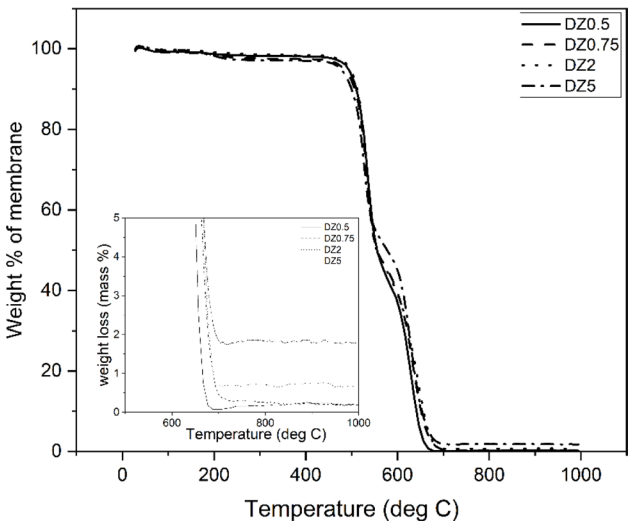

Fig. 2 Thermal degradation of PSF/ZIF-8 MMMs in presence of air.

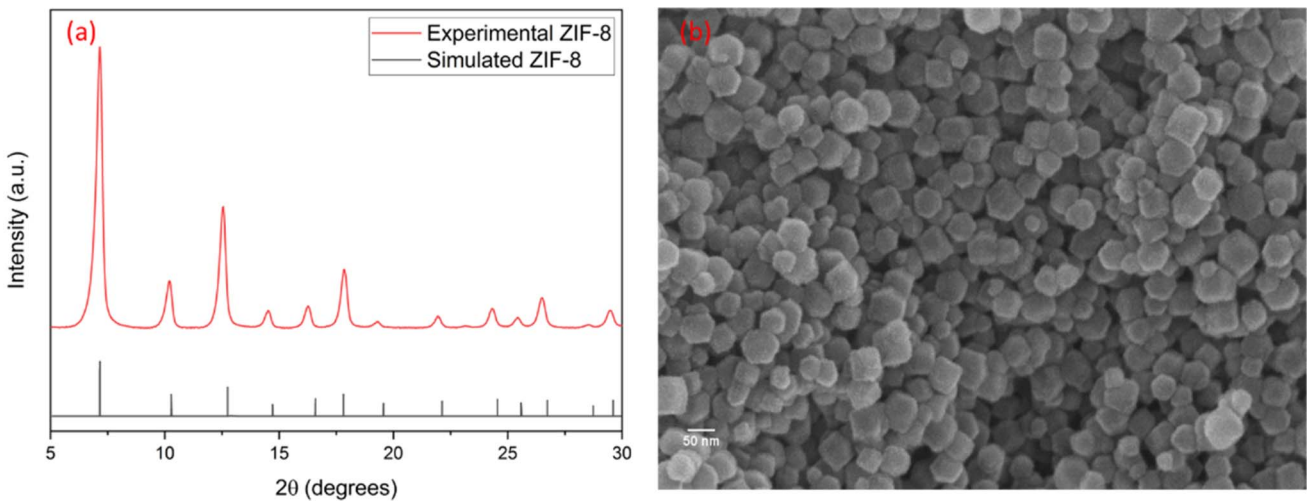

Fig. 1 Characterization of ZIF-8 (a) X-ray diffraction peaks (b) scanning electron microscope micrograph.

Table 2 ZIF-8 loading for different mixed matrix membranes as calculated from TGA and EDS

	Loading (weight%)			
Membrane	Experimental	TGA	EDS (whole)	EDS (agglomerate)
DZ0.5	0.50	0.44	0.49	—
D0.75	0.75	0.54	0.70	—
DZ2	2.00	1.91	2.56	4.17
DZ5	5.00	5.06	7.33	8.07

thermal stability of particles by thermogravimetry. A known amount of synthesized nanoparticles were placed in a Teflon pan and heated from 30 °C to 1000 °C at a heating rate of 10 °C min^{-1}. Gas sorption analysis of the ZIF-8 particles was done in presence of N_2 using Autosorb iQ instrument. The analysis was performed at 77 K after a pretreatment in vacuum for about 4 hours.

The morphology of pure polysulfone as well as MMMs were determined using a JEOL-JSM 7600F FEGSEM after sputter coating the samples with platinum. EDS was also carried out in the same equipment for elemental mapping across the membrane surface. The samples were prepared by cutting a small piece from the membrane with a sharp blade in a single cut. NETZSCH STA Luxx analyser was used for determining the thermal stability of membranes. A known quantity of synthesized nanoparticles was placed in a Teflon pan and heated from 30 °C to 1000 °C at a heating rate of 10 °C min^{-1}.

2.4.2 Gas permeation experiments. The gas permeation experiments were conducted in a lab-scale setup (used in our previous study[29] also) equipped for measuring the permeation of both pure as well as mixed gases. The experiments were repeated using three different membrane samples in order to check the reproducibility of data. The setup was designed as described elsewhere in the literature.[30] Further details are given in ESI and Fig. S1† shows the schematic diagram of the setup.

3. Results and discussion

3.1 Filler characterization

The XRD pattern of ZIF-8 is shown in Fig. 1a. The characteristic peaks for ZIF-8 are present at 2θ values of 7.3, 10.35, 12.7, 14.8, 16.4, 18, 22.1, 23.9 and 26.5, and are well in agreement with the simulated ZIF-8 peaks and with the literature.[28,31,32] The FEG-SEM micrograph for ZIF-8 is shown Fig. 1b where the rhombic dodecahedron morphology of the ZIF-8 particles is clearly visible. A similar particle shape for ZIF-8 has been reported in the literature.[31,33,34] The formation of phase-pure ZIF-8 may therefore be concluded. The particle size of synthesized ZIF-8 is around 40 nm. Since the dense membranes have thickness of 25–30 microns, the filler particles are easily accommodated within the membrane thickness. TGA analysis of ZIF-8 was done from 29 °C to 1000 °C in a flow of nitrogen. The weight loss profile with temperature is shown in Fig. S2 (ESI†). Thermal degradation of ZIF-8 starts at around 350 °C and continues till 600 °C after which the weight becomes constant at around 30% of the initial weight, that corresponds to ZnO. Similar behaviour has also been reported in literature.[25]

The sorption isotherm using N_2 gas in Fig. S3 (ESI†) shows a type I isotherm with a hysteresis around a relative pressure of 1 indicating that the sample is microporous. The surface area is 1176 m^2 g^{-1} (BET method) and average pore volume is 0.706 cm^3 g^{-1} and of 0.452 cm^3 g^{-1}. Cravillon *et al.* have reported BET surface area of 960 m^2 g^{-1} and micropore volume of 0.36 cm^3 g^{-1}.[28] Other literature reports the values that are in the range of what is observed experimentally in this study.[35] It should be

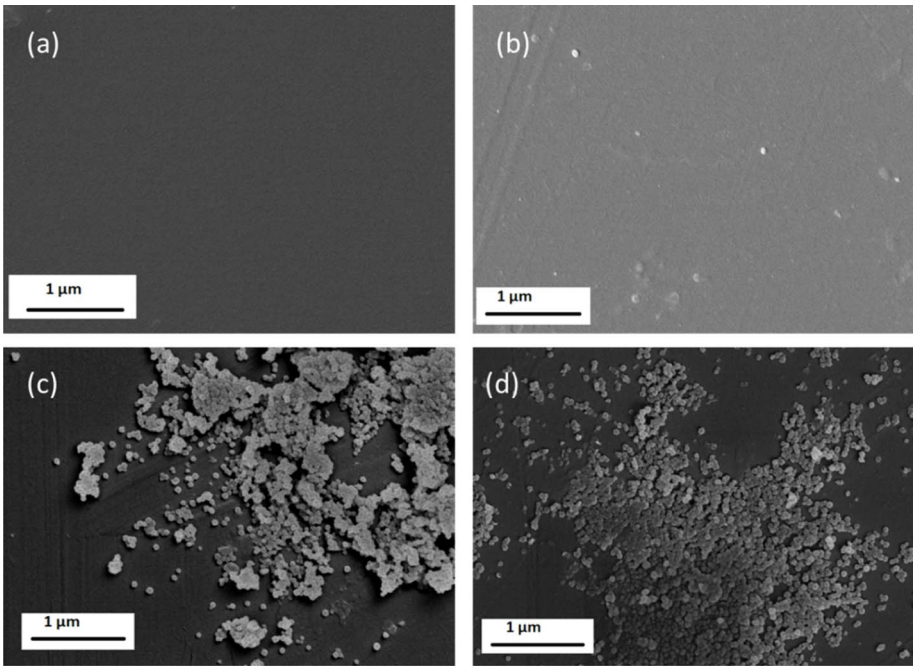

Fig. 3 SEM micrographs for dense PSF/ZIF-8 mixed matrix membranes (a) DZ0.75 (b) DZ1 (c) DZ2 (d) DZ5.

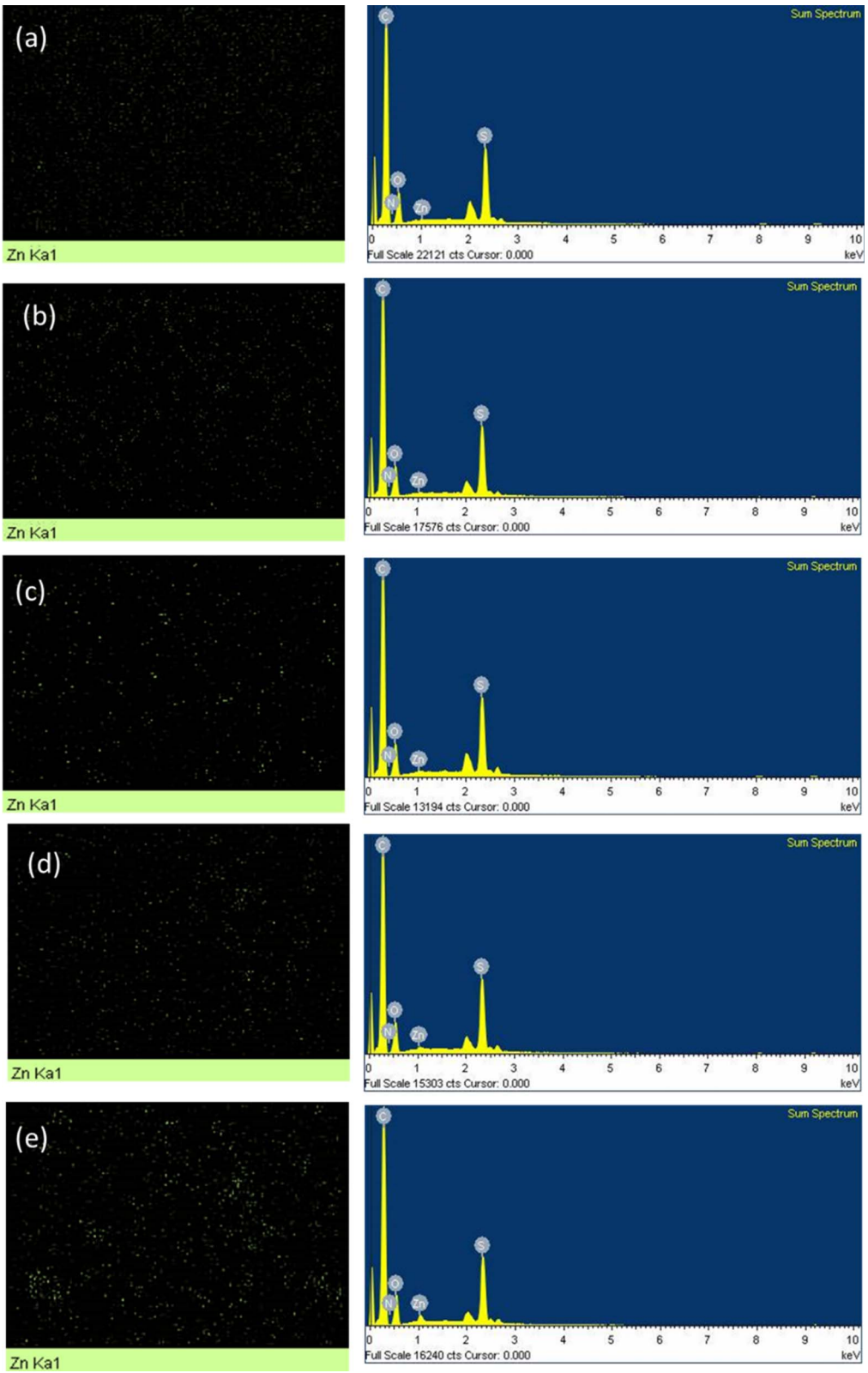

Fig. 4 EDS analysis showing an increase in Zn content with ZIF-8 loading for PSF/ZIF-8 MMMs (a) DZ0.5 (b) DZ0.75 (c) DZ1 (d) DZ2 (e) DZ5.

noted that any difference that are present can be attributed to different synthesis and pretreatment conditions involved in the analysis. This high surface area and microporosity suggests that ZIF-8 can enhance the gas sorption when used in the polymer matrix. The sorption isotherm with CO_2 in Fig. S4† show that ZIF-8 has an adsorption capacity of 16.37 $cm^3\ g^{-1}$ for CO_2 at

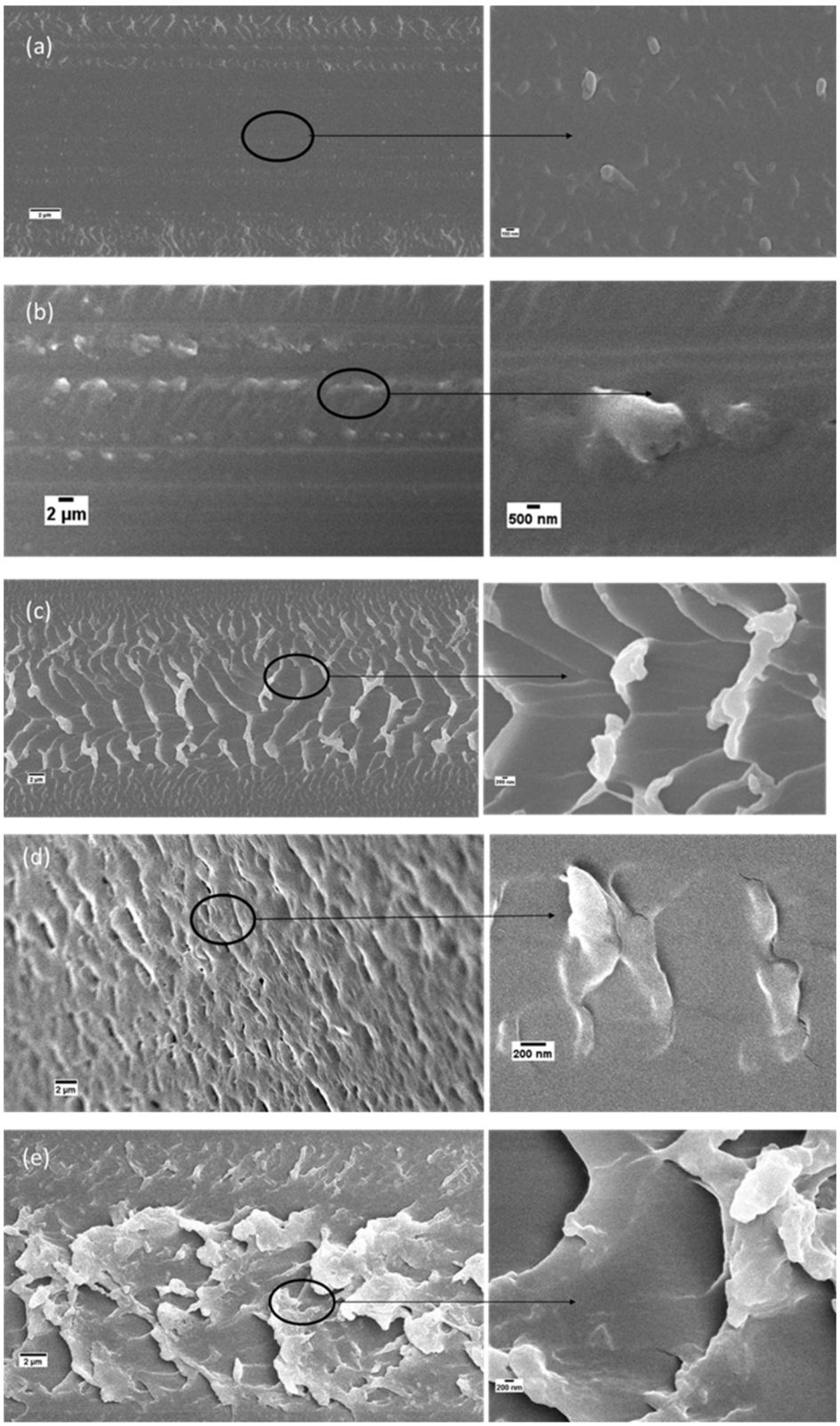

Fig. 5 SEM micrographs (cross section) for dense PSF/ZIF-8 mixed matrix membranes (a) DZ0.5 (b) DZ0.75 (c) DZ1 (d) DZ2 (e) DZ5. The panels on the right show the circled regions from the corresponding panels on the left at a higher magnification.

a pressure of around 1 bar (temperature 298 K). This affinity for CO_2 suggests that ZIF-8 is suitable as a filler in mixed matrix membranes to enhance the separation properties.

3.2 Membrane characterization

Thermal degradation behaviour of MMMs is shown in Fig. 2 from room temperature (29 °C) to 1000 °C in a flow of oxygen. It

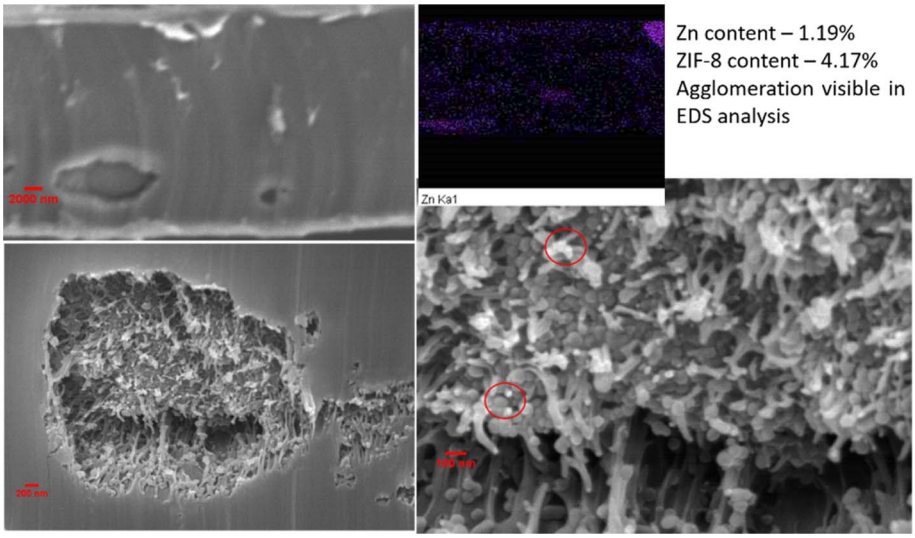

Fig. 6 Cross sectional micrographs of DZ2 membrane showing agglomeration and EDS analysis showing ZIF-8 particles agglomeration (red circles).

was observed that the membranes are stable till a temperature of 450 °C, the temperature at which degradation of polysulfone begins; all the polymer is lost by 600 °C. It can be observed in the inset of Fig. 2 that the residual weight of membrane increases with increase in loading of the filler.

The ZIF-8 content in the membrane was estimated from the residual weight in the TGA experiments and the results are listed in Table 2. It was observed that the membranes show a loading close to the experimental loading.

Surface images of the dense membranes are shown in Fig. 3 for the membranes DZ0.75, DZ1, DZ2 and DZ5. The membranes show a homogeneous surface and no defects are visible on the membrane. A significant agglomeration is seen for membranes DZ2 and DZ5 (Fig. 3c and d respectively). Agglomeration of particles in dense membranes have also been reported in the literature for MMMs[18,36] and it may prove as a hindrance to gas transport through the membranes as the surface area available for gas permeation decreases.

To check for the presence of any interfacial voids at polymer–particle interfaces, imaging was done for the DZ5 membrane that has the highest loading of ZIF-8. The image, shown in Fig. S4 (ESI†), shows no interfacial defects that could result in non-selective transport in the membranes. The characteristic shape of ZIF-8 particles is also discernible in this image.

Fig. 4 shows the elemental analysis of the membranes, carried out in EDS mode of FESEM. The membranes at lower loadings show a comparatively homogenous dispersion of particles whereas at higher loadings some agglomeration is

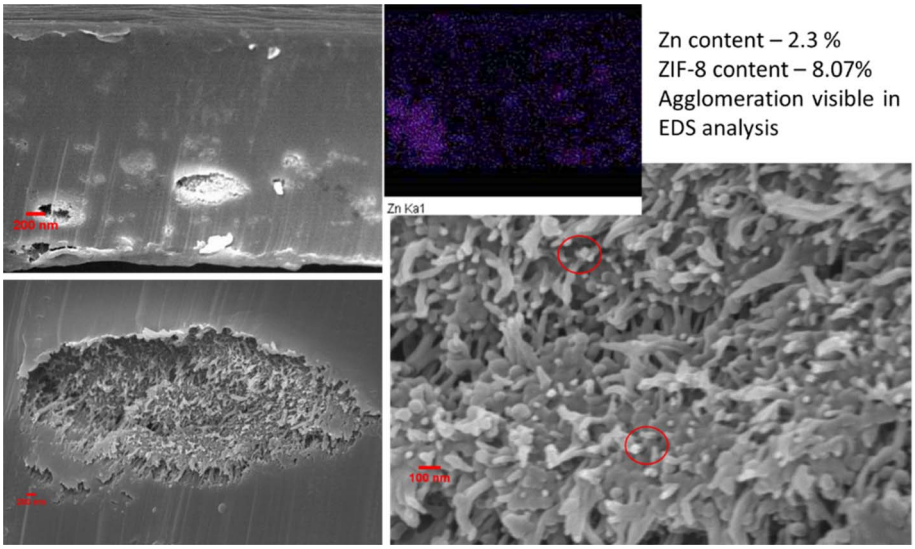

Fig. 7 Cross sectional micrographs of DZ5 membrane showing agglomeration and EDS analysis showing ZIF-8 particles agglomeration (red circles).

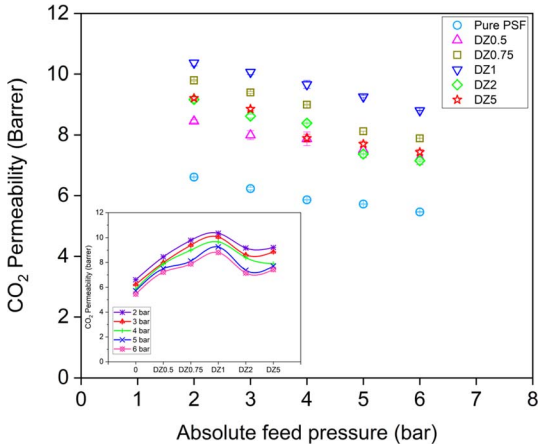

Fig. 8 CO_2 permeability of dense PSF/ZIF-8 mixed matrix membranes at different loadings of ZIF-8. Pure PSF results are also shown for comparison. Inset shows the permeabilities plotted as a function of loading for different pressures.

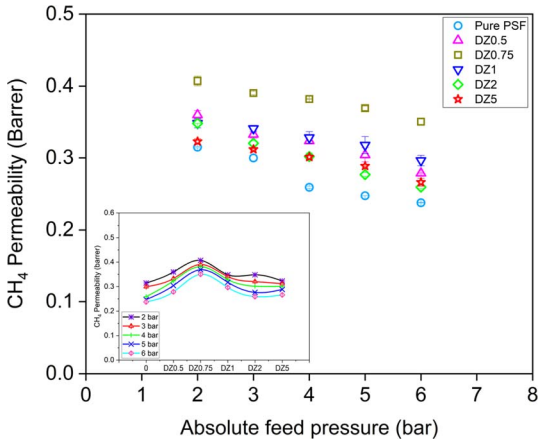

Fig. 9 CH_4 permeability of dense PSF/ZIF-8 mixed matrix membranes at different loadings of ZIF-8. Pure PSF results are also shown for comparison inset shows the permeabilities plotted as a function of loading for different pressures.

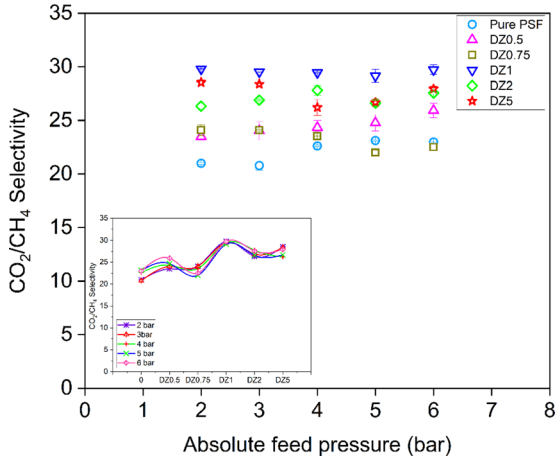

Fig. 10 CO_2/CH_4 selectivity of dense PSF/ZIF-8 mixed matrix membranes at different loadings of ZIF-8. Pure PSF results are also shown for comparison. Inset shows the selectivity plotted as a function of loading for different pressures.

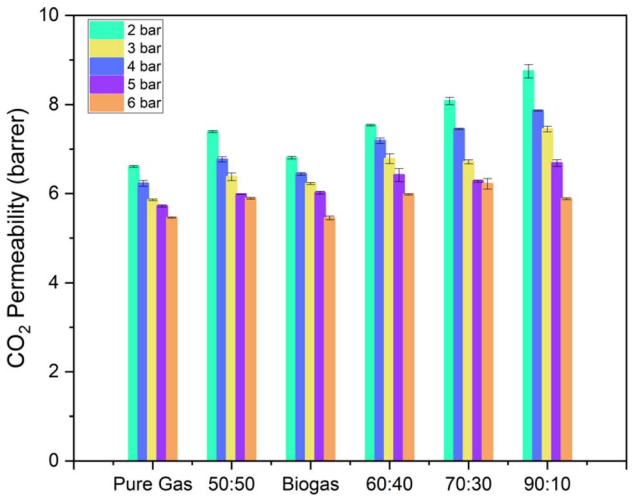

Fig. 11 CO_2 permeability of pure PSF membranes for mixed gas (CH_4 and CO_2) in different ratios (shown in x-axis are CH_4 : CO_2 ratio). Pure gas results are also shown for comparison.

visible as observed in earlier micrographs also. A small peak of Zn in the spectra is visible that increases in size with increase in ZIF-8 loading.

The percentage loading (weight% of ZIF-8 in membrane matrix) was also calculated from elemental analysis (EDS) at higher loadings (where such quantification was possible) and it was found that the calculated values are close to the loading as per the recipe employed, as shown in Table 2.

Cross-sectional SEM micrographs were also used to ascertain the distribution of ZIF-8 across the thickness of the MMMs and also to check for agglomeration tendencies. For this purpose, the membrane samples were sandwiched between two layers of resin, microtomed and observed under the microscope. The micrographs are shown in Fig. 5, and show a tendency towards agglomeration at ZIF-8 loading of higher than 0.75%.

Elemental mapping was done for the membranes DZ2 (see Fig. 6) and DZ5 (see Fig. 7) as the higher loading in these membranes makes detection possible by EDS analysis. It is observed that, while the ZIF-8 particles are distributed throughout the thickness, some agglomeration is visible at several locations. The amount of ZIF-8 calculated is around 4 wt%, and 8 wt%, which is higher than the actual loading of 2 wt% and 5 wt% in the membranes respectively. This ZIF-8 loading on the membrane surface for DZ2 and DZ5 membrane was 2.56 wt% and 7.33 wt%, much less than in the cross-section. The agglomeration of particles is one of the major problems that has been known to deteriorate membrane permeability due to blocked passages for the gas transport.

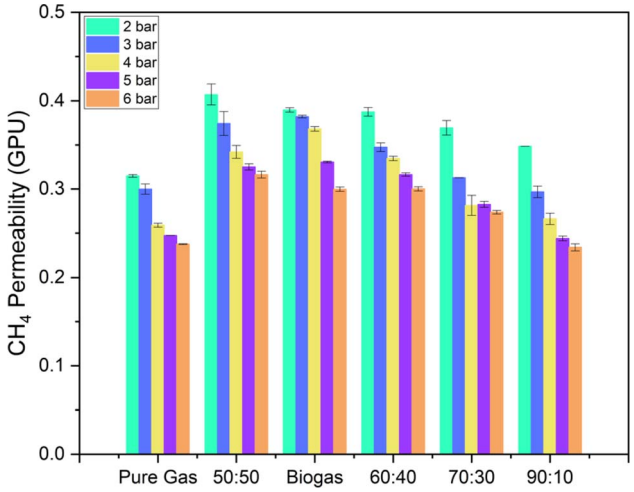

Fig. 12 CH_4 permeability of pure PSF membranes for mixed gas (CH_4 and CO_2) in different ratios (shown in *x*-axis are CH_4 : CO_2 ratio). Pure gas results are also shown for comparison.

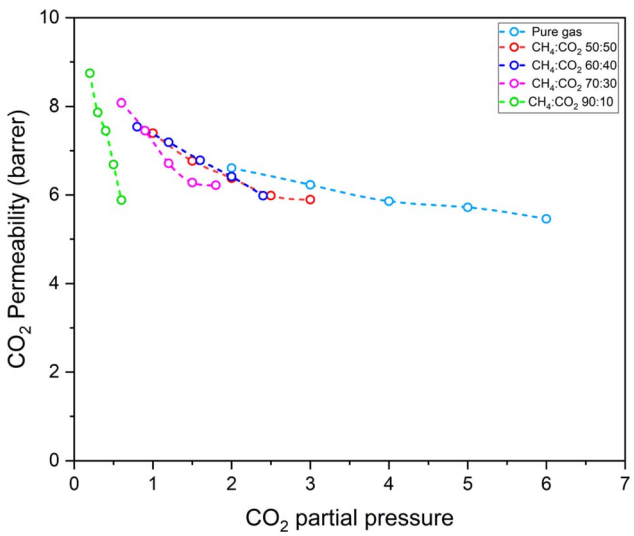

Fig. 13 CO_2 permeability of pure PSF membranes for mixed gas (CH_4 and CO_2) in different ratios. Pure gas results are also shown for comparison.

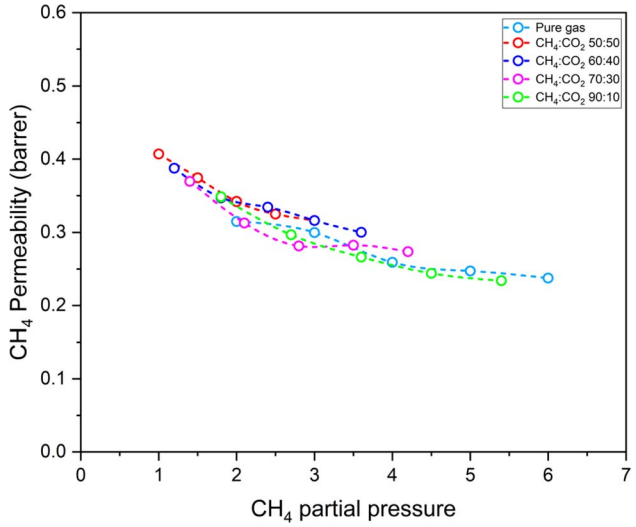

Fig. 14 CH_4 permeability of pure PSF membranes for mixed gas (CH_4 and CO_2) in different ratios. Pure gas results are also shown for comparison.

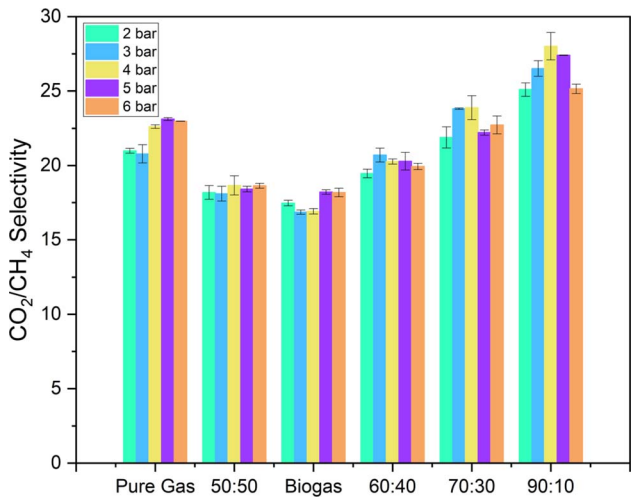

Fig. 15 CO_2/CH_4 selectivity of pure PSF membranes for mixed gas (CH_4 and CO_2) in different ratios (shown in *x*-axis are CH_4 : CO_2 ratio). Pure gas results are also shown for comparison.

3.3 Gas permeation studies

The permeation behaviour of PSF as well as PSF/ZIF-8 MMMs were studied over a feed pressure range of 2 to 6 bar for pure and mixed gases. Membrane performance was also studied with raw biogas feed, with composition: CH_4 (45%), CO_2 (44%), N_2 (10%) and O_2 (~3%), H_2S (800 ppm). The biogas composition analysis was done in COMBIMASS® portable gas analyser. Since the analyser is not equipped for N_2 detection, it was done using gas chromatography. In this section, we discuss the results.

3.3.1 Pure gas permeation studies. The permeability values of pure CO_2 and CH_4 with increasing feed pressure for pure polysulfone and MMMs with different loadings of ZIF-8 are shown in Fig. 8 and 9. The CO_2 and CH_4 permeability values decrease with increasing pressure for pure PSF as well as mixed matrix membranes. This is in accordance with the behaviour of glassy polymers[37–40] and can be explained by the Dual Mode Sorption model where the Langmuir sorption sites tend to saturate at lower pressure thereby decreasing the permeability at higher pressures.

As Fig. 8 shows (also see the inset), the CO_2 permeability values for all MMMs are higher than those for pure PSF membranes, indicating that ZIF-8 particles enhance the CO_2 transport through the membranes. This enhancement is attributed to the affinity of ZIF-8 for CO_2; researchers have also invoked, as an explanation for the increase in permeability, the pore size of ZIF-8 (3.4 Å), which is higher than the kinetic diameter of CO_2 molecule (3.3 Å).[23,41] However, as the inset

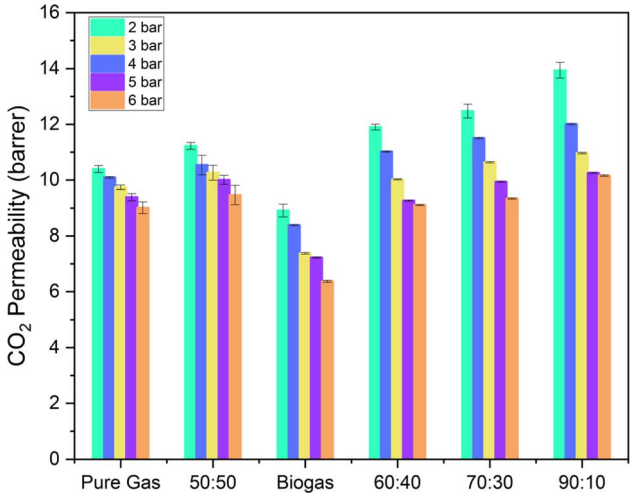

Fig. 16 CO_2 permeability of DZ1 MMMs for mixed gas (CH_4 and CO_2) in different ratios (shown in x-axis are CH_4 : CO_2 ratio). Pure gas results are also shown for comparison.

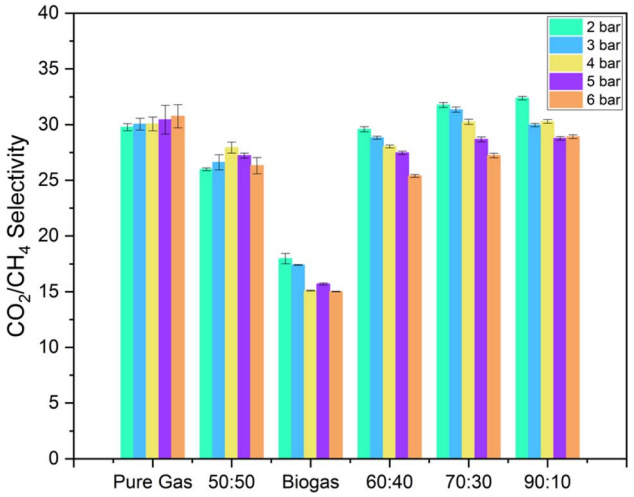

Fig. 18 CO_2/CH_4 selectivity of DZ1 MMMs for mixed gas (CH_4 and CO_2) in different ratios (shown in x-axis are CH_4 : CO_2 ratio). Pure gas results are also shown for comparison.

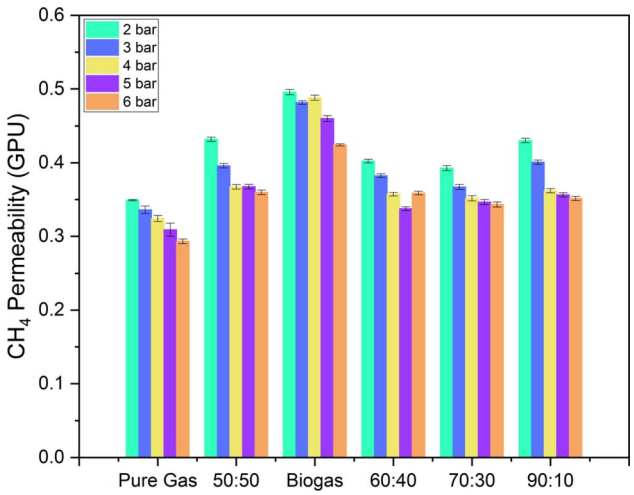

Fig. 17 CH_4 permeability of DZ1 MMMs for mixed gas (CH_4 and CO_2) in different ratios (shown in x-axis are CH_4 : CO_2 ratio). Pure gas results are also shown for comparison.

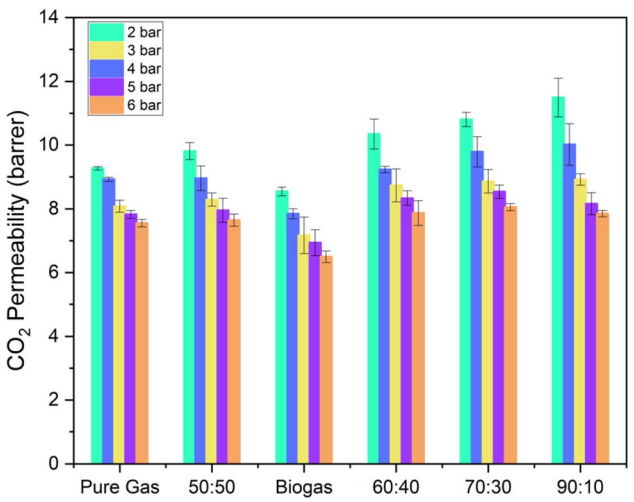

Fig. 19 CO_2 permeability of DZ5 MMMs for mixed gas (CH_4 and CO_2) in different ratios (shown in x-axis are CH_4 : CO_2 ratio). Pure gas results are also shown for comparison.

shows clearly, the permeability increase for CO_2 with loading starts to decrease beyond 1%. The highest increase in permeability is observed for DZ1 membrane, and is 56.8% compared to pure PSF. At loadings higher than 1 wt%, a decrease in membranes permeability is observed. The agglomeration of ZIF-8 particles on the membrane surface results in blockage of channels for gas flow thereby reducing the permeability.

Fig. 9 shows similar data for methane permeation through pure PSF and mixed matrix membranes. An increase in permeability of methane is also observed for MMMs (although less than for CO_2), ranging from 3 to 35% for different loadings. While the transport of CH_4 through the pores of ZIF-8 is restricted *via* size sieving due to its larger diameter, the modest increase observed may be because of some tendency of CH_4 to adsorb on ZIF-8.[42,43] In this case also, the permeability goes through a maximum, but at a lower loading (0.75%) than in the case of CO_2. This may be because methane is larger in size than CO_2, because of which its permeability reduces even for 1 wt% loading where very less agglomeration is seen.

Fig. 10 shows the selectivity values of the dense pure PSF and PSF/ZIF-8 MMMs as a function of feed gas pressure. The selectivity of the MMMs is higher than that of pure PSF membranes, and generally increases with increase in ZIF-8 loading, suggesting that ZIF-8 not only has the potential of improving the CO_2 permeability but also CO_2/CH_4 selectivity. The highest increase of 42% in selectivity is observed for the membrane DZ1 whereas for DZ5 membrane the selectivity increases by 36%.

3.3.2 Mixed gas permeation studies. The results on pure gas permeation showed that, among the membranes tested, the

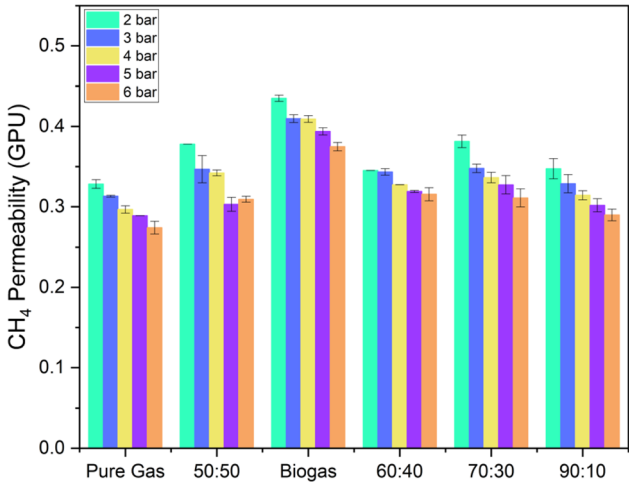

Fig. 20 CO_2 permeability of DZ5 MMMs for mixed gas (CH_4 and CO_2) in different ratios (shown in x-axis are CH_4 : CO_2 ratio). Pure gas results are also shown for comparison.

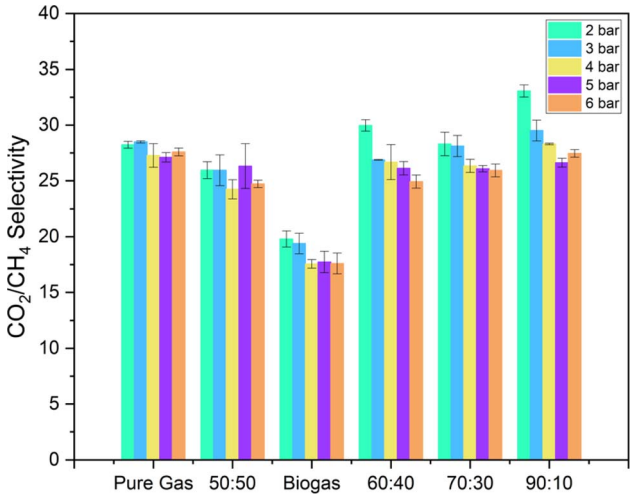

Fig. 21 CO_2/CH_4 selectivity of DZ5 MMMs for mixed gas (CH_4 and CO_2) in different ratios. Pure gas results are also shown for comparison.

membrane DZ1 had the highest increases in CO_2 permeability and CO_2/CH_4 selectivity. DZ5, with the highest loading of ZIF-8, also showed a considerable increase in selectivity like DZ1. So, these membranes were selected for studies on mixtures of CO_2 and CH_4. To demonstrate the advantages of MMMs, it is necessary to first go through the performance of pure PSF membranes for mixed gases.

Fig. 11 and 12 show the variation in permeability for gas mixtures of different compositions, along with biogas, at different pressures for CO_2 and CH_4 respectively. For each composition, it is observed that the membrane permeability decreases with the increase in pressure that is expected phenomena for glassy polymers as explained in Section 3.3.1.

A comparison between permeabilities at particular pressure sheds light into how the membrane performance changes with composition of the gas. The results indicate an increase in CO_2 permeability with a decrease in CO_2 content of the feed gas at the same total pressure. The increase in permeability for feed gas containing 50%, 40%, 30% and 10% CO_2 are 12%, 14.24%, 22.4% and 32.4% respectively, compared to pure gas values. This may seem as an advantage in the stagewise enrichment of the mixture, since the leaner the mixtures get in CO_2, the faster does the latter permeate, but a much lower increment of 2.99% in CO_2 permeability for biogas is recorded (compared to what is expected from made-up mixtures under similar conditions). For CH_4, the permeability is higher in mixed gases than for pure gas and decreases with a decrease in methane content of the gas. The increase in CH_4 permeability for feed gas containing 50%, 40%, 30% and 10% CO_2 is 29%, 22.8%, 17.14% and 10.47% respectively. Here, biogas shows a little lower increment of 3% in CH_4 permeability (lower than that seen for a made-up mixture with similar composition). The minor components of biogas may contribute to a reduction in permeance of the major constituents, depending on their affinity to the polymer membrane.

These findings are of obvious relevance to the design of membrane cascades for biogas enrichment, in which the permeate streams are progressively treated for recovery of methane while the retentate streams are treated for further enrichment of methane.

Glassy polymeric membranes are expected to show a competitive sorption effect where the presence of other components in the mixture decreases the availability of sorption sites for a given gas, thus reducing its permeability. To analyse the effect of competition, the permeabilities for CO_2 and CH_4 are plotted against their respective partial pressures in Fig. 13 and 14 respectively. It is observed that, for the same overall driving force for transport, CO_2 permeability is the lesser, the lesser its content in the mixture, with $CH_4 : CO_2$ having 90 : 10 composition showing the least permeability. This cannot be explained as a partial pressure effect by the tenets of dual model sorption and can only be explained as the effect of competition – the passage of CO_2 through the membranes is hindered by the presence of methane. However, the results for methane, shown in Fig. 14, show much less of an effect of competition; no significant change is seen in methane permeability for the same feed partial pressure, in mixtures as compared to pure gas.

The selectivity values of pure PSF membranes for mixed gases is shown in Fig. 15. The selectivity values of mixed gas with $CH_4 : CO_2$ of 70 : 30 and 90 : 10 is higher than the pure gas selectivity due to a greater increase in CO_2 permeance than that of CH_4 whereas the selectivity of $CH_4 : CO_2$ of 60 : 40 and 50 : 50 is lower than the pure gas values. The highest selectivity is observed at a pressure of 4 bar for $CH_4 : CO_2$ of 90 : 10 mixed gas. For biogas, the selectivity values of the membranes are lower than the ideal selectivity and mixed gas selectivity due to a higher increase in CH_4 permeability as compared to CO_2 permeability. This study suggests that polysulfone membranes suffer a loss in selectivity and permeability with gas mixtures as compared to the pure component values (even more so with biogas).

The behaviour of MMMs with mixed gas feeds will now be discussed further. Fig. 16 shows the CO_2 permeability values for DZ1 membrane. As in the case of pure PSF membranes, CO_2 permeability increases with decrease in CO_2 content in the feed at the same total pressure. The increase in permeability for feed gas containing 50%, 40%, 30% and 10% CO_2 are 7.97%, 14.49%, 20.1% and 34.07% respectively, compared to pure gas values. For biogas, the CO_2 permeability was 14.26% lower than with pure gas values and 20.58% lower than artificial gas mixture with similar CO_2 composition. While this behaviour is qualitatively similar to what was observed for pure PSF membrane, the MMM shows higher permeability than pure PSF membranes at all compositions. Thus, the enhancement in CO_2 permeability of DZ1 membranes from pure PSF membranes for feed gas containing 50%, 40%, 30% and 10% CO_2 is 51.75%, 57.82%, 54.4% and 59.39% respectively at a total feed pressure of 2 bar, while at the same pressure, the CO_2 permeability increased by 30.6% for biogas. The lowering of permeability for biogas indicates competitive sorption effects by the other (minor) components present.

For CH_4 permeation in DZ1 membrane, as shown in Fig. 17, permeability values in mixtures are higher than for pure methane. The increase in CH_4 permeability for feed gas containing 50%, 40%, 30% and 10% CO_2 is 23.73%, 15.22%, 12.49% and 23.27% respectively. For biogas, an increase of 42.06% from the pure gas values and 14.81% from the artificial mixture with similar composition is observed. The increase in CH_4 permeability of DZ1 membranes from pure PSF membranes for feed gas containing 50%, 40%, 30% and 10% CO_2 is 6.13%, 3.81%, 6.31% and 23.53% respectively at 2 bar total feed pressure. With biogas, the CH_4 permeability shows an increase of 53.31% as compared to pure PSF membranes. As the CH_4 content increases, the permeability values decrease with $CH_4 : CO_2$ in 50 : 50 ratio showing the highest CH_4 permeability, this behaviour being the same as for pure PSF membranes. The CH_4 permeability in the case of biogas shows the highest increment from all the mixed gas values.

For biogas, a higher decrease in CO_2 permeability and increase in CH_4 permeability from the pure gas values is observed as compared to pure PSF membranes. The presence of ZIF-8 in the MMMs may be responsible for such behaviour. The surface degradation of ZIF-8 on exposure to acidic gases like H_2S has been reported in the literature[42,44] with the development of cavities in some cases.[43] A small increase in CO_2 and CH_4 uptake is also reported for ZIF-8 nanoparticles in the presence of H_2S.[42] However, a decrease in the diffusivity of CO_2 is also reported due to development of a surface barrier that is created in ZIF-8 on exposure to acidic gases such as H_2S. It appears that this combined effect on diffusivity and uptake is responsible for the decrease in CO_2 permeability. Since ZIF-8 does not allow passage of CH_4 an increased uptake results in increased permeability.

Selectivity values of DZ1 membranes for mixed gases is shown in Fig. 18. The selectivity values of mixed gas with $CH_4 : CO_2$ of 70 : 30 and 90 : 10 is higher than the pure gas selectivity due to the greater increase in CO_2 permeability than that of CH_4, whereas the selectivity for 60 : 40 and 50 : 50 mixtures is lower than the ideal selectivity with pure gases. A larger decrease in selectivity is seen for biogas, due to lower CO_2 permeability and higher methane permeability. The selectivity values for MMMs is higher than for pure polysulfone membrane at all pressures studied. This is because of the higher increase in CO_2 permeability as compared to methane due to presence of ZIF-8 in mixed matrix membranes.

DZ5 membranes were also studied with the same gas mixtures as DZ1 MMMs. The trends of permeability from pure gas to mixed gas in mixed matrix membranes were the same as DZ1 membranes. The variation of CO_2 permeability, CH_4 permeability and CO_2/CH_4 selectivity for DZ5 membranes are shown in Fig. 19–21.

Though the DZ5 membranes showed considerable enhancement in permeability as compared with the pure polysulfone membranes for both pure and mixed gases, the CO_2 and CH_4 permeability were lower for DZ5 membranes as compared to DZ1 membranes. This is due to the agglomeration of particles at higher loading that can be seen in scanning electron micrographs (see Fig. 6). This agglomeration of particles leads to blockage of channels thereby restricting the amount of gas that should pass through them if there is no agglomeration. The selectivity values are similar to the DZ1 membrane; this is the result of similar decreases in CO_2 and CH_4 permeability.

4. Conclusions

While mixed matrix membranes for gas separations have been considered for over a decade now, the research has mostly been focused on development of novel fillers that show potential for enhancement of membrane permeability and selectivity, based on pure gas experiments. The present work is focused on mixed matrix membranes with ZIF-8 as a filler at various loadings, with the efficacy of the membranes being studied for separation of mixed gases (of different proportions of CO_2 and CH_4), as well as biogas, in addition to pure gas. MMMs generally show a higher permeability and CO_2/CH_4 selectivity, the highest increments being 56.8% and 41% respectively for the membrane with 1 wt% loading of ZIF-8. A decrease in performance at higher loadings (while these were still superior to pure PSF) is possibly because of the tendency of the filler particles to agglomerate. With gas mixtures too, MMMs were found to show increased permeability and selectivity than the pure PSF membranes for all gaseous mixture. With the change in feed gas composition, it was observed that the CO_2 permeability increased with the increase in CO_2 content of the feed gas. The effect of gas composition on permeability, at the same feed partial pressure, indicates significant competitive effects for CO_2, while the same are negligible in the case of CH_4. These results have obvious implications in staged enrichment of gas mixtures, as the mixture composition changes from one stage to the next.

With biogas as feed, these membranes showed a 14.6% decrease in CO_2 permeability and a 39.64% decrease in ideal selectivity from the as compared to pure gas values. These values are much lower for those observed with binary mixture containing equivalent ratio of CO_2 and CH_4. This difference in

behaviour has been attributed to the presence of H_2S in the real biogas; H_2S is known to degrade the ZIF-8 structure thereby reducing the CO_2 permeability.

These studies suggest that the performance of ZIF-8 MMMs is superior to pure polysulfone membranes. However, a loss of both permeability and selectivity is observed when binary gas mixtures are used. Their performance suffers further when biogas is used as a feed as compared to pure gases. With an increase in filler loading, agglomeration tends to take place thereby restricting further enhancements in permeability and selectivity. The use of ZIF-8 as filler in MMMs for biogas enrichment would require methods for reducing agglomeration at higher loadings so that full potential of ZIF-8 can be exploited.

The work highlights the potential of ZIF-8 in improving the permeability as well as selectivity of pure polysulfone membranes for removal of carbon dioxide from gas mixtures, and in particular for the upgradation of biogas to biomethane. The data on mixtures, such as generated in this paper is of obvious importance in the design of membrane cascades. In a forthcoming part of the study, we examine the behaviour of dense MMMs in the light of known theories of membrane and effective medium transport.

Data availability

The data recorded in this manuscript is available on request.

Conflicts of interest

There are no conflicts to declare.

References

1 M. Miltner, A. Makaruk and M. Harasek, Review on available biogas upgrading technologies and innovations towards advanced solutions, *J. Clean. Prod.*, 2017, **161**, 1329–1337.
2 A. I. Adnan, M. Y. Ong, S. Nomanbhay, K. W. Chew and P. L. Show, Technologies for biogas upgrading to biomethane: a review, *Bioengineering*, 2019, **6**(4), 1–23.
3 E. Ryckebosch, M. Drouillon and H. Vervaeren, Techniques for transformation of biogas to biomethane, *Biomass Bioenergy*, 2011, **35**(5), 1633–1645.
4 D. Andriani, A. Wresta, T. D. Atmaja and A. Saepudin, A review on optimization production and upgrading biogas through CO 2 removal using various techniques, *Appl. Biochem. Biotechnol.*, 2014, **172**(4), 1909–1928.
5 L. Yang, X. Ge, C. Wan, F. Yu and Y. Li, Progress and perspectives in converting biogas to transportation fuels, *Renew. Sustain. Energy Rev.*, 2014, **40**, 1133–1152.
6 Q. Sun, H. Li, J. Yan, L. Liu, Z. Yu and X. Yu, Selection of appropriate biogas upgrading technology-a review of biogas cleaning, upgrading and utilisation, *Renew. Sustain. Energy Rev.*, 2015, **51**, 521–532.
7 V. Vrbová and K. Ciahotný, Upgrading Biogas to Biomethane Using Membrane Separation, *Energy Fuels*, 2017, **31**(9), 9393–9401.
8 R. Kadam and N. L. Panwar, Recent advancement in biogas enrichment and its applications, *Renew. Sustain. Energy Rev.*, 2017, **73**, 892–903.
9 R. W. Baker, Future directions of membrane gas separation technology, *Ind. Eng. Chem. Res.*, 2002, **41**(6), 1393–1411.
10 L. M. Robeson, Correlation of separation factor versus permeability for polymeric membranes, *J. Membr. Sci.*, 1991, **62**(2), 165–185.
11 L. M. Robeson, The upper bound revisited, *J. Membr. Sci.*, 2008, **320**(1–2), 390–400.
12 D. R. Paul and D. R. Kemp, The diffusion time lag in polymer membranes containing adsorptive fillers, *J. Polym. Sci., Polym. Symp.*, 1973, **93**(41), 79–93.
13 M. Vinoba, M. Bhagiyalakshmi, Y. Alqaheem, A. A. Alomair, A. Pérez and M. S. Rana, Recent progress of fillers in mixed matrix membranes for CO2separation: a review, *Sep. Purif. Technol.*, 2017, **188**, 431–450.
14 M. Rezakazemi, A. Ebadi Amooghin, M. M. Montazer-Rahmati, A. F. Ismail and T. Matsuura, State-of-the-art membrane based CO2 separation using mixed matrix membranes (MMMs): an overview on current status and future directions, *Prog. Polym. Sci.*, 2014, **39**(5), 817–861.
15 M. Vinoba, M. Bhagiyalakshmi, Y. Alqaheem, A. A. Alomair, A. Pérez and M. S. Rana, Recent progress of fillers in mixed matrix membranes for CO2 separation: a review, *Sep. Purif. Technol.*, 2017, **188**, 431–450.
16 S. Sorribas, B. Zornoza, C. Téllez and J. Coronas, Mixed matrix membranes comprising silica-(ZIF-8) core-shell spheres with ordered meso-microporosity for natural- and bio-gas upgrading, *J. Membr. Sci.*, 2014, **452**, 184–192.
17 A. Nuhnen, M. Klopotowski, H. B. Tanh Jeazet, S. Sorribas, B. Zornoza, C. Téllez, *et al.*, High performance MIL-101(Cr) @6FDA-: M PD and MOF-199@6FDA- m PD mixed-matrix membranes for CO2/CH4 separation, *Dalton Trans.*, 2020, **49**(6), 1822–1829.
18 M. Z. Ahmad, V. Martin-Gil, V. Perfilov, P. Sysel and V. Fila, Investigation of a new co-polyimide, 6FDA-bisP and its ZIF-8 mixed matrix membranes for CO2/CH4 separation, *Sep. Purif. Technol.*, 2018, **207**, 523–534.
19 T. Rodenas, M. V. Dalen, P. Serra-Crespo, F. Kapteijn and J. Gascon, Mixed matrix membranes based on NH_2-functionalized MIL-type MOFs: influence of structural and operational parameters on the CO_2/CH_4 separation performance, *Microporous Mesoporous Mater.*, 2014, 35–42.
20 C. Wu, K. Zhang, H. Wang, Y. Fan, S. Zhang, S. He, *et al.*, Enhancing the gas separation selectivity of mixed-matrix membranes using a dual-interfacial engineering approach, *J. Am. Chem. Soc.*, 2020, **142**(43), 18503–18512.
21 A. F. Bushell, M. P. Attfield, C. R. Mason, P. M. Budd, Y. Yampolskii, L. Starannikova, *et al.*, Gas permeation parameters of mixed matrix membranes based on the polymer of intrinsic microporosity PIM-1 and the zeolitic imidazolate framework ZIF-8, *J. Membr. Sci.*, 2013, **427**, 48–62.
22 N. A. H. M. Nordin, A. F. Ismail, A. Mustafa, R. S. Murali and T. Matsuura, The impact of ZIF-8 particle size and heat

treatment on CO2/CH4 separation using asymmetric mixed matrix membrane, *RSC Adv.*, 2014, **4**(94), 52530–52541.

23 N. A. H. M. Nordin, A. F. Ismail, A. Mustafa, R. S. Murali and T. Matsuura, Utilizing low ZIF-8 loading for an asymmetric PSf/ZIF-8 mixed matrix membrane for CO_2/CH_4 separation, *RSC Adv.*, 2015, **5**(38), 30206–30215.

24 I. U. Khan, M. H. D. Othman, A. Jilani, A. F. Ismail, H. Hashim, J. Jaafar, *et al.*, ZIF-8 based polysulfone hollow fiber membranes for natural gas purification, *Polym. Test.*, 2020, **84**, 106415.

25 B. Sasikumar, S. Bisht, G. Arthanareeswaran, A. F. Ismail and M. H. D. Othman, Performance of polysulfone hollow fiber membranes encompassing ZIF-8, SiO2/ZIF-8, and amine-modified SiO2/ZIF-8 nanofillers for CO2/CH4 and CO2/N2 gas separation, *Sep. Purif. Technol.*, 2021, **264**, 118471.

26 H. J. Kim and S. I. Hong, The sorption and permeation of CO2 and CH4 for dimethylated polysulfone membrane, *Korean J. Chem. Eng.*, 1997, **14**(3), 168–174.

27 K. Ghosal, R. T. Chern, B. D. Freeman, W. H. Daly and I. I. Negulescu, Effect of basic substituents on gas sorption and permeation in polysulfone, *Macromolecules*, 1996, **29**(12), 4360–4369.

28 M. Wiebcke, J. Cravillon, S. Münzer, S. J. Lohmeier, A. Feldhoff, K. Huber, *et al.*, Rapid Room-Temperature Synthesis and Characterization of Nanocrystals of a Prototypical Zeolitic Imidazolate Framework, *Chem. Mater.*, 2009, **21**(8), 1410–1412.

29 S. Negi and A. K. Suresh, Thermodynamic Aspects of Membrane Synthesis: Application to Biogas Enrichment, *Ind. Eng. Chem. Res.*, 2023, **62**(37), 15120–15135.

30 O. C. David, D. Gorri, A. Urtiaga and I. Ortiz, Mixed gas separation study for the hydrogen recovery from H2/CO/N2/CO2 post combustion mixtures using a Matrimid membrane, *J. Membr. Sci.*, 2011, **378**(1–2), 359–368.

31 Z. Si, D. Cai, S. Li, G. Li, Z. Wang and P. Qin, A high-efficiency diffusion process in carbonized ZIF-8 incorporated mixed matrix membrane for n-butanol recovery, *Sep. Purif. Technol.*, 2019, **221**, 286–293.

32 K. S. Park, Z. Ni, A. P. Côté, J. Y. Choi, R. Huang, F. J. Uribe-Romo, *et al.*, Exceptional chemical and thermal stability of zeolitic imidazolate frameworks, *Proc. Natl. Acad. Sci. U. S. A.*, 2006, **103**(27), 10186–10191.

33 N. A. H. M. Nordin, A. F. Ismail and A. Mustafa, Synthesis and preparation of asymmetric PSf/ZIF-8 mixed matrix membrane for CO2/CH4 separation, *J. Teknol.*, 2014, **69**(9), 73–76.

34 M. Balçık, S. B. Tantekin-Ersolmaz and M. G. Ahunbay, Interfacial analysis of mixed-matrix membranes under exposure to high-pressure CO2, *J. Membr. Sci.*, 2020, **607**, 118147.

35 Y. Zhang, Y. Jia, M. Li and L. Hou, Influence of the 2-methylimidazole/zinc nitrate hexahydrate molar ratio on the synthesis of zeolitic imidazolate framework-8 crystals at room temperature, *Sci. Rep.*, 2018, **8**(1), 1–7.

36 N. Jusoh, Y. F. Yeong, K. K. Lau and A. M. Shariff, Transport properties of mixed matrix membranes encompassing zeolitic imidazolate framework 8 (ZIF-8) nanofiller and 6FDA-durene polymer: optimization of process variables for the separation of CO2from CH4, *J. Cleaner Prod.*, 2017, **149**, 80–95.

37 W. J. Koros, D. R. Paul and A. A. Rocha, Carbon Dioxide Sorption and Transport in Polycar bonate, *J. Polym. Sci.*, 1976, **14**, 687–702.

38 W. J. Koros, Model for Sorption of Mixed Gases in Glassy Polymers, *J. Polym. Sci., Part A-2*, 1980, **18**(5), 981–992.

39 W. J. Koros, R. T. Chern, V. Stannett and H. B. Hopfenberg, Model for Permeation of Mixed Gases and Vapors in Glassy Polymers, *J. Polym. Sci., Part A-2*, 1981, **19**(10), 1513–1530.

40 G. Liu, Y. Labreche, V. Chernikova, O. Shekhah, C. Zhang, Y. Belmabkhout, *et al.*, Zeolite-like MOF nanocrystals incorporated 6FDA-polyimide mixed-matrix membranes for CO2/CH4 separation, *J. Membr. Sci.*, 2018, **565**, 186–193.

41 M. J. C. Ordoñez, K. J. Balkus, J. P. Ferraris and I. H. Musselman, Molecular sieving realized with ZIF-8/Matrimid® mixed-matrix membranes, *J. Membr. Sci.*, 2010, **361**(1–2), 28–37.

42 A. Dutta, N. Tymińska, G. Zhu, J. Collins, R. P. Lively, J. R. Schmidt, *et al.*, Influence of Hydrogen Sulfide Exposure on the Transport and Structural Properties of the Metal-Organic Framework ZIF-8, *J. Phys. Chem. C*, 2018, **122**(13), 7278–7287.

43 S. Reljic, A. Broto-Ribas, C. Cuadrado-Collados, E. O. Jardim, D. Maspoch, I. Imaz, *et al.* - 2020 - Reljic - Structural Deterioration of Well-Faceted MOFs upon H2S Exposure and its Effect in the Adsorption Performance, *Chem.–Eur. J.*, 2020, 17110–17119.

44 C. Han, C. Zhang, N. Tymińska, J. R. Schmidt and D. S. Sholl, Insights into the Stability of Zeolitic Imidazolate Frameworks in Humid Acidic Environments from First-Principles Calculations, *J. Phys. Chem. C*, 2018, **122**(8), 4339–4348.